Food Chemistry: X 21 (2024) 101064

Contents lists available at ScienceDirect

Food Chemistry: X

journal homepage: www.sciencedirect.com/journal/food-chemistry-x

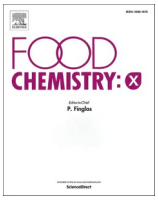

Effect of modified okara insoluble dietary fibre on the quality of yoghurt

Yu Tian [a], Yanan Sheng [a], Tong Wu [a], Changyuan Wang [a,b,*]

[a] College of Food, Heilongjiang Bayi Agricultural University, Xinfeng Lu 5, Daqing 163319, PR China
[b] Chinese National Engineering Research Center, Daqing 163319, PR China

ARTICLE INFO

Keywords:
Functional yoghurt
Modification
Okara insoluble dietary fibre
Stability

ABSTRACT

The aim of this study was to investigate the potential of adding soya bean dregs insoluble dietary fibre (IDF) modified by jet cavitation combined with cellulase to yoghurt to improve its functional properties (Yoghurt was prepared by adding 10 μL of yoghurt fermenter to 100 mL of milk, fermented to pH 4.5 in a constant temperature incubator at 42 °C, and then stored in a refrigerator at 4 °C after adding IDF separately). The results showed that the modified IDF had a rough structure with high water-holding capacity and sodium cholate adsorption capacity. The addition of modified IDF improved the pH, hardness, and elasticity of the yoghurt. During the entire storage period, the titratable acidity and whey precipitation rate of the modified IDF yoghurt gradually increased, and antioxidant activity gradually decreased, and its titratable acidity, whey precipitation rate, and antioxidant activity had a significant advantage compared with those of the blank group yoghurt. In conclusion, the modified soya bean dregs IDF-added yoghurt prepared by jet cavitation combined with the cellulase method has the potential for sodium cholate adsorption capacity and antioxidant activity, which can confer unique functional properties and improve the pH, texture, and reduce whey precipitation of yoghurt. This study provides a scientific basis for the application of soya bean dregs IDF as a fibre fortifier in yoghurt production and suggests innovative ideas for the design of functional dairy products.

1. Introduction

Dietary fibre (DF) is a carbohydrate that cannot be digested or absorbed by the human body, but still offers numerous health benefits (Cui et al., 2019). DF is classified into two categories based on its water solubility, soluble dietary fibre (SDF) and insoluble dietary fibre (IDF) (Dong et al., 2021). The appropriate intake of IDF is crucial for improving digestive tract health, reducing blood lipids, regulating blood sugar levels, and controlling body weight (Tian et al., 2022). IDF can be extracted from several agro-industrial products and added to food matrices to produce IDF-rich foods that provide new choices for health-conscious consumers (Luo et al., 2018). However, its addition negatively affects the colour, flavour, and texture of the final functional food (Zhou et al., 2020). Therefore, modifying IDF to overcome its shortcomings and expand its application in the food industry are challenges that need to be overcome. Physical, chemical, enzymatic, and microbial fermentation methods can be used to improve IDF properties (Gan et al., 2021).

Jet cavitation is widely used as a physical processing method in other industries because of its simple operation, short processing time, and low cost, and it has demonstrated potential for applications in food processing. Accordingly, it can improve the structural and functional properties of soybean proteins, such as their solubility and emulsification, and the physical and chemical properties of okara DF (Wu et al., 2021; Wu et al., 2020). Importantly, the enzymatic modification of IDF alone might be insufficient because the tight structure of IDF limits the ability of the enzyme to fully contact the cellulose and hemicellulose. Thus, compared to the use of a single method, a combined modification method can merge the advantages of two methods, avoid the disadvantages of a single modification, and be used to prepare high-quality modified IDF according to the characteristics of the raw materials. As such, a combination of enzymatic and physical methods is ideal for modifying IDF. For example, Zhu et al. (2022) treated sea buckthorn IDF with ball milling combined with cellulase, which changed the microstructure through the protection of its main components. Compared to

Abbreviations: IDF, insoluble dietary fibre; DF, dietary fibre; SDF, soluble dietary fibre; F-IDF, unmodified IDF; M−IDF, cavitation jet combined with cellulase modified IDF; FY, yogurt with F-IDF; MY, yogurt with M−IDF; AOAC, Association of Official Agricultural Chemists; WHC, water-holding capacity; OHC, oil-holding capacity; SC, swelling capacity; SEM, scanning electron microscope; FT-IR, Fourier transform infrared spectroscopy; SAC, sodium cholate adsorption capacity; TA, titratable acidity.

* Corresponding author.
E-mail address: byndwcy@163.com (C. Wang).

https://doi.org/10.1016/j.fochx.2023.101064
Received 16 October 2023; Received in revised form 26 November 2023; Accepted 11 December 2023
Available online 14 December 2023

those with the pure ball milling method, the water- and oil-holding, glucose-adsorption, and cholesterol-adsorption capacities and swelling performance of the combined modified IDF were improved, and we previously reached a similar conclusion (Tian et al., 2023).

Yoghurt is a fermented dairy product. Increased yoghurt intake is associated with high dietary quality and nutritional value, improved human gastrointestinal health, and a reduced risk of several diseases. However, plain yoghurt lacks various nutrients including DF, flavonoids, and iron. Recently, the addition of DF to yoghurt has improved its texture and stability (Fan et al., 2023). Qin et al. (2023) applied ultrafine milling combined with *Lactobacillus paracasei*-modified teak peel SDF to yoghurt and found that the gel strength and hardness of the yoghurt were improved, and it had stronger odour characteristics. Kumanri et al. (2023) added cellulase and xylanase-modified pea peel DF to yoghurt and the results of the study showed that the gel strength and whey precipitation rate of yoghurt were reduced with the increase of the concentration of DF. We found that modified okara IDF has better water-holding capacity (WHC), hypoglycaemic effects, and *in vitro* fermentation ability (Tian et al., 2023). However, to date, there have been no studies on yoghurt containing IDF before and after jet cavitation combined with cellulase modification. Herein, we used jet cavitation combined with cellulase-modified okara IDF and studied the effects on the microstructure, rheological properties, and storage stability of yoghurt, before and after this modification. A theoretical basis is also provided for the development of functional foods rich in IDF.

2. Materials and methods

2.1. Materials

Dried okara (51.8 g·100 g^{-1} dietary fibre, 19.32 g·100 g^{-1} protein) was procured from Kedong Yuwang Soybean Protein Food Co., Ltd. (Qiqihaer, China). Skim milk (3.2 g·mL^{-1} protein, 4.8 g·mL^{-1} carbohydrate, and 4.0 g·mL^{-1} fat) was obtained from Inner Mongolia Mengniu Dairy Co., Ltd. (Neimenggu, China). A freeze-dried probiotic culture (1.0 L) containing a mixture of Lactobacillus bulgaricus, Streptococcus thermophilus, Lactobacillus acidophilus, Lactobacillus plantarum, and Lactobacillus casei was obtained from Beijing Chuanxiu Technology Co. (Beijing, China); food-grade neutral protease (enzyme activity $\geq$ 1000 U/g) was obtained from Dingzhou Bexis Biotechnology Co., Ltd. (Hebei, China); and food-grade cellulase (enzyme activity $\geq 1 \times 10^4$ U/g) was from Henan Wanbang Chemical Technology Co., Ltd. (Henan, China); other reagents were food-grade.

2.2. F-IDF and M−IDF preparation from okara

F-IDF was prepared according to the method described by Wu et al. (2020) with the following modifications: ten grams of okara powder were mixed with 400 mL of distilled water and boiled for 10 min. After removing impurities, the mixture was cooled to 60 °C, and the pH was adjusted to 7.0. One hundred microliters of protease was added, and hydrolysis was performed at 45 °C. The enzyme was then heat-inactivated, and the sample was further cooled to 25 °C. The sediment was collected by centrifugation at 8000 rpm for 20 min at 4 °C using a centrifuge (H2500R, Hunan Xiangyi Laboratory Instrument Development Co., Ltd., China), washed with 95 % food-grade ethanol and acetone, and dried in an oven at 60 °C to a constant weight. The resulting product was named F-IDF.

To prepare M−IDF, F-IDF was dissolved in water (1:20, w/v) at 20 °C and subjected to jet cavitation treatment for 90 min at 0.5 MPa. The sample solution was collected and heated in a water bath at 50 °C. The pH was adjusted to 5.0, and 400 μL of cellulase was added for enzymatic hydrolysis for 30 min. At the end of the digestion, cellulase was inactivated using a water bath (HH-6, Jiangsu Dongpeng Instrument Manufacturing Co., Ltd., China) at 95 °C, and the precipitate was collected by centrifugation at 8000 rpm for 20 min at 4 °C using a centrifuge (H2500R, Hunan Xiangyi Laboratory Instrument Development Co., Ltd., China). The precipitate was dried in an oven at 60 °C to a constant weight, resulting in M−IDF (Tian et al., 2023).

2.3. Component analysis

The IDF yields were determined using the method of Tian et al. (2023). The moisture content was determined using the Association of Official Agricultural Chemists (AOAC) method 925.40, until the sample attained a constant weight at 105 °C. The crude protein content of the fibre samples was measured using the AOAC method 950.40, using a Kjeldahl apparatus. Based on AOAC method 920.39, the crude fat content in the sample was determined via Soxhlet extraction.

2.4. Monosaccharide composition

To determine the monosaccharide composition of IDF samples, a method modified by Xi et al. (2023) was used. IDF (20 mg) was hydrolysed with 2 mL of 2 M trifluoroacetic acid at 100 °C for 8 h. After cooling to room temperature, the hydrolysate was evaporated and dissolved in 2.0 mL of distilled water. The solution was then mixed with 0.3 M NaOH and 0.5 M (PMP) methanol solution at a ratio of 1:3:2 and allowed to react at 70 °C for 1 h. After neutralisation with 0.6 mL of 0.3 M HCl, the solution was extracted three times with 3 mL of chloroform. The resulting solutions were filtered through a 0.22 μm microporous membrane and analysed using high-performance liquid chromatography (LC-20AD; Kishimazu Corporation, Tokyo, Japan) with a Wondastl C18 (4.6 mm × 200 mm, 5 μm) column. The column temperature was set to 30 °C, and the injection volume was 20 μL. The mobile phase was potassium dihydrogen phosphate acetonitrile solution (pH 6.7) at a flow rate of 1.0 mL/min.

2.5. Scanning electron microscope (SEM) evaluations

The surface morphology of the freeze-dried samples was observed using SEM (SU8020, Hitachi, Japan). Prior to testing, 2 mg of the sample was weighed and fixed on a metal plate using an electrical adhesive, and a thin gold layer was spray-plated under vacuum for 60 s. Scanning images were taken at an accelerating voltage of 3 kV and magnifications from 2000 × to 5000× (Lyu et al., 2021).

2.6. Fourier transform infrared spectroscopy (FT-IR)

The functional groups present in the samples were analysed using a Nicolet 5700 FT-IR spectrometer (Nicolet IS10, Nicolet, USA). Samples containing KBr particles (Sample: KBr = 1 mg:100 mg) were immediately placed in an optical path and scanned 32 times in the range of 4000–500 cm^{-1} with a resolution of 4 cm^{-1} to obtain an infrared spectrum (Luo et al., 2018).

2.7. Functional properties of okara IDF

To determine the WHC, the IDF was weighed and 30 mL of distilled water was added. The mixture was shaken well and then centrifuged at 4000 rpm for 10 min at 4 °C using a centrifuge (H2500R, Hunan Xiangyi Laboratory Instrument Development Co., Ltd., China). The supernatant was discarded and the remaining solid was weighed (Sang et al., 2022). WHC was calculated as follows:

$$WHC(g/g) = \frac{A_2 - A_1}{IDFdryweight(g)}$$

A_1 is the weight of IDF and centrifuge tube (g); A_2 is the weight of IDF after absorbing water and the centrifuge tube (g).

To determine the oil-holding capacity (OHC), 1 g of IDF was weighed and 30 mL of soybean oil was added. The mixture was shaken, allowed to stand for 1 h at room temperature, centrifuged at 4000 rpm for 10 min

at 4 °C using a centrifuge (H2500R, Hunan Xiangyi Laboratory Instrument Development Co., Ltd., China), and the supernatant was discarded (Tian et al., 2023). OHC was calculated as follows:

$$OHC(g/g) = \frac{A_2 - A_1}{IDFdryweight(g)}$$

A_1 is the weight of IDF and the centrifuge tube (g); A_2 is the weight of IDF after oil absorption and the centrifuge tube (g).

To determine the swelling capacity (SC), 0.5 g of IDF was weighed and 35 mL of distilled water was added, shaken evenly, and allowed to stand for 18 h at room temperature (Si et al., 2023). SC was calculated as follows:

$$SC(mL/g) = \frac{A_2 - A_1}{IDFdryweight(g)}$$

A_1 is the volume of the sample before swelling (mL); A_2 is the volume of the sample after swelling (mL).

To determine the sodium cholate adsorption capacity (SAC) of IDF, 0.2 g of IDF and 0.1 g of sodium cholate were dissolved in 25 mL of 0.15 M NaCl, and the reaction was carried out using a thermostatic shaker (KT-80A, Changzhou Zhongbei Instrumentation Co. Ltd., China) for a sustained period of 4 h at 37 °C. The reaction was carried out at 4 °C for 20 min. At the end of the reaction, 1 mL of the supernatant was mixed with 1 mL of 0.3 % furfural and 6 mL of 45 % H_2SO_4 in a glass tube after centrifugation at 4000 rpm for 20 min at 4 °C using a centrifuge (H2500R, Hunan Xiangyi Laboratory Instrument Development Co., Ltd., China). The mixture was then placed in a water bath (HH-6, Jiangsu Dongpeng Instrument Manufacturing Co., Ltd., China) at 65 °C for 30 min. The absorbance was measured at 620 nm using a UV spectrophotometre (752 N, Shanghai Yidian Analytical Instruments Co., Ltd., China), and the standard curve for sodium cholate was y = 0.22x + 0.0052, R^2 = 0.997 (Yang et al., 2021). The SAC was calculated as follows:

$$SAC(g/g) = \frac{A_2 - A_1}{IDFdryweight(g)}$$

A_1 is the sodium cholate content in the solution after adsorption (mg/L), and A_2 is the sodium cholate content in the solution before adsorption (mg/L).

2.8. Yoghurt preparation

Functional yoghurt containing IDF was prepared according to Wang et al. (2020) to produce functional yoghurt samples, named FY, MY 0.1 %, MY 0.5 %, and MY 1.0 %. Yoghurt without IDF was used as the control. Yoghurt samples were then stored at 4 °C in a refrigerator in the dark for analysis, and the pH, titratable acidity (TA), and whey separation rate on days 1, 7, 14, and 21 were determined.

2.9. Determination of total and reducing sugar content of yoghurt after different storage periods

The total sugar content in each sample was determined via the phenol–sulfuric acid method (Tian et al., 2023). Yoghurt samples were removed from the refrigerator at 4 °C and centrifuged at 8000 rpm for 10 min at 4 °C using a centrifuge (H2500R, Hunan Xiangyi Laboratory Instrument Development Co. Ltd., China). The yoghurt supernatant was diluted 1000-fold, and 0.2 mL of the diluted solution was placed in a dry and clean test tube. Then, 0.8 mL distilled water, 1 mL 95 % phenol solution, and 5 mL concentrated sulphuric acid were added and left to stand for 10 min. The mixture was then mixed using a vortex shaker (UVS-1, Beijing Yusheng United Science and Technology Co., Ltd., China). Ltd., China) at 30 °C for 20 min. After the reaction, the mixture was cooled to room temperature at 25 °C, and the absorbance was measured at 490 nm using a UV spectrophotometre (752 N, Shanghai Yidian Analytical Instrument Co., Ltd., China). The standard curve of total sugar was $y = 0.0078x + 0.0722$ ($R^2 = 0.996$).

The reducing sugar content in each sample was determined via the DNS comparison method (Tian et al., 2023). Yoghurt samples were removed from the refrigerator at 4 °C and centrifuged at 8000 rpm for 10 min at 4 °C using a centrifuge (H2500R, Hunan Xiangyi Laboratory Instrument Development Co., Ltd., China). The yoghurt supernatant was diluted 10 times, and 0.2 mL of the diluted solution was placed in a dry, clean test tube. Then, 0.5 mL distilled water and 2.5 mL DNS were added and mixed using a vortex shaker (UVS-1, Beijing Yusheng United Technology Co., Ltd., China), and the mixture was placed in a water bath (HH-6, Jiangsu Dongpeng Instrument Manufacturing Co., Ltd., China) at 100 °C for 5 min. After the reaction, the solution was cooled to room temperature (25 °C), 10 mL of distilled water was added, and absorbance was measured at 540 nm using a UV spectrophotometre (752 N, Shanghai Yidian Analytical Instruments Co., Ltd., China). The standard curve for the reducing sugars was $y = 1.5053x$-0.023 ($R^2 = 0.998$).

2.10. pH, TA, and whey precipitation rate determination

The pH of the yoghurt samples was determined using a pH meter (FE28, Mettler-Toledo International Co., Ltd., Shanghai, China) after 1, 7, 14, and 21 days of storage at 4 °C. Control and IDF-containing yoghurt were diluted twice with water to determine the TA. The diluted yoghurt was titrated with 0.1 M NaOH to a pH of 8.0 ± 0.1. The values were calculated in g of lactic acid per 100 g of yoghurt as follows:

$$TA\,(\%) = (f^*V^*0.9)/W$$

W is the initial mass of yoghurt, f is the molar concentration of NaOH, V is the volume of 0.1 mol/L NaOH, and 0.9 is the scaling parameter of lactic acid.

The yoghurt whey isolation rate was measured according to the method described by Miocinovic et al. (2018). 15 g of yoghurt was using a centrifuge (H2500R, Hunan Xiangyi Laboratory Instrument Development Co., Ltd., China) at 3000 rpm for 15 min at 4 °C and the supernatant was collected, and the resulting supernatant was weighed. Whey precipitation was calculated as follows:

$$Wheyprecipitationrate\,(\%) = (W_y/W_S) \times 100\%$$

W_y is the weight of the supernatant, and W_s is the weight of the yoghurt.

2.11. Colour measurement

Colour was measured using a colourimeter (Konica Minolta CM-700d, Japan) with whiteboard corrections before use. Data were expressed as a*(+a* = redness and − a* = greenness), L* (L* = 100 [white] and L* = 0 [black]), or b* (+b* = yellowness and − b* = blueness) (Sang et al., 2022). Additionally, the hue and chroma were calculated as follows:

$$Hue = \arctan(b^*/a^*)$$

$$Chroma = \sqrt{(a^{*2} + b^{*2})}$$

2.12. Rheological test

Rheological tests were performed as described by Dong et al. (2018), using an MCR92 rheometer (Anton Paar Trading Co., Ltd., Shanghai, China). The steady-state viscosity of the stirred yoghurt sample was measured at shear rates of 1 to 100 s^{-1}. Before the time sweep test of the elastic modulus, a 100 s^{-1} rotating shear rate was applied to all samples, and the yoghurt structure recovery was obtained at 4 °C for 2 h. The tests were performed under a constant strain of 0.5 % and a frequency of 1 Hz. A frequency sweep test was then performed at frequencies ranging from 0.1 Hz to 100 Hz. The storage (G′) and loss moduli (G″) were monitored during the tests.

2.13. Texture testing

The yoghurt texture (hardness, springiness, cohesiveness, and gumminess) was determined according to the method described by Miocinovic et al. (2018). A texture analyser (Universal TA-2019, Shanghai Tengba Instrument Technology Co., Ltd., Shanghai, China) was used with minor modifications. Yoghurt was placed in a 60 mm × 70 mm (diameter × height) dish and transferred to a measuring table. The test parameters were the P/50 cylindrical probe diameter (3.6 mm), test speed (1.0 mm/s [front], 1.0 mm/s [middle], 2.0 mm/s [back]), and test distance (20 mm). The compression degree and measurement temperature were set at 20 mm and 15 °C, respectively.

2.14. Organoleptic investigation

The sensory evaluation used in this study was approved by the Institutional Review Board of Heilongjiang Bayi Nongken University. The organoleptic characteristics of yoghurt were assessed by 30 professionally trained personnel (15 males and 15 females) based on four different quality characteristics, specifically colour, taste, odour, and state of organisation (Table 1).

2.15. Determination of antioxidant capacity

2.15.1. Determination of DPPH• scavenging capacity

Yoghurt samples were removed from the refrigerator at 4 °C, and the supernatant was collected after centrifugation at 8000 rpm for 10 min at 4 °C using a centrifuge (H2500R, Hunan Xiangyi Laboratory Instrument Development Co. Ltd., China). The DPPH• solution was prepared at a concentration of 0.06 mmol/L. The solution was prepared in 0.2 mL ethanol. Ethanol (0.2 mL) was added to the DPPH• solution (4 mL) as a blank, and the initial absorbance was measured at 517 nm using a UV spectrophotometre (752 N, Shanghai Yidian Analytical Instruments Co., Ltd., China). DPPH• solution (4 mL) was mixed with 0.2 mL of supernatant and incubated for 1 h. The absorbance was measured at 517 nm using a UV spectrophotometre (752 N, Shanghai Yidian Analytical Instruments Co., Ltd., China) and recorded as A_p. A mixture of ethanol (4 mL) and 0.2 mL of supernatant was used as a control group, and absorbance was recorded as A_c. The measurements were performed three times in parallel, and the average value was taken (Lyu et al., 2021). The free radical scavenging rate formula is as follows:

Table 1
Sensory rating scale.

Project	Marking criterion	Score
Colour	Yoghurt uniform colour, lustre, easy to accept	20–15
	Yoghurt colour is darker or lighter, uniform colour, dark colour, easier to accept	14–6
	Yoghurt colour is not uniform, has no lustre, not easy to be accepted	5–0
Form of organization	The texture is uniform, with no whey precipitation, moderate viscosity, no bubbles	20–15
	The texture is uniform, with whey precipitation, a small amount of bubbles, moderate viscosity	14–6
	The texture is not uniform, the amount of whey precipitation is large, too thick or too thin, and the amount of bubbles is large	5–0
Odour	It has a typical yoghurt aroma and a pleasant smell	20–15
	The flavour of yoghurt is lighter, with no smell	14–6
	No typical yoghurt aroma, not an acceptable smell	5–0
Taste	The taste is delicate, sweet and sour, easy to accept	20–15
	The taste is more delicate, sweet and sour moderate, and more acceptable	14–6
	Rough taste, sweet and sour, not easy to accept	5–0
Overall acceptability	Fully accept	20–15
	Generally, accept	14–6
	More acceptable	5–0

$$scavengingrate(\%) = \frac{A_0 - A_P - A_C}{A_0} \times 100$$

2.15.2. Determination of ABTS •+ scavenging ability

A 7 mmol/L ABTS•$^+$ solution and a 2.45 mmol/L potassium persulfate solution were prepared, mixed at the same volume ratio, and allowed to stand in the dark for 12 h. ABTS•$^+$ solution was obtained by dilution with distilled water, and the absorbance at 732 nm was 0.700 ± 0.20 using a UV spectrophotometre (752 N, Shanghai Yidian Analytical Instruments Co., Ltd., China). The ABTS•$^+$ solution (4 mL) was added to 200 μL of the yoghurt supernatant. The solution was mixed thoroughly and incubated in the dark at 25 °C for 6 min. The absorbance of the reaction mixture was measured at 734 nm using a UV spectrophotometre (752 N, Shanghai Yidian Analytical Instruments Co., Ltd., China). Control samples were prepared according to the methods described above without any extract. The free radical scavenging ability of each test sample was measured by the reduction of ABTS•$^+$ absorbance (Lyu et al., 2021) and calculated using the following equation:

$$scavengingrate(\%) = \frac{A_{control} - A_{sample}}{A_{control}} \times 100$$

2.15.3. Determination of total antioxidant capacity (T-AOC)

Total antioxidant capacity was determined using a reference kit (Nanjing Jiancheng Bioengineering Institute Co., Ltd., Jiangsu, China). Under acidic conditions, antioxidants can reduce Fe^{3+}-TPTZ to produce blue Fe^{2+}-TPTZ, the change in colour of which can be detected at 593 nm. Therefore, the total antioxidant capacity of the sample was calculated from the change in absorbance.

2.16. Statistical analysis

All the experiments were repeated three times unless stated otherwise. The results are reported as means ± standard deviation. Statistical analysis was carried out using SPSS Statistics 27 (IBM, USA). Statistical significance was determined at $P < 0.05$. Data were analysed using one-way ANOVA followed by a Tukey test.

3. Results and discussion

3.1. Analysis of IDF yield, composition, and monosaccharide composition

The yield and composition of IDF extracted using different methods were similar, but there were some differences (Table 2). Compared with that of F-IDF, the M−IDF yield was reduced, mainly because IDF was partly converted into SDF via jet cavitation combined with cellulase treatment. There were significant differences in the protein content between the two IDFs ($P < 0.05$).

The monosaccharide composition of F-IDF and M−IDF was determined to clarify the effects of jet cavitation combined with cellulase treatment on IDF. Pectin is the main component of IDF, and its components, such as galactose, arabinose, rhamnose, and galacturonic acid, account for a large proportion (Table 2). The galactose content was the highest and was the main monosaccharide in okara IDF. The galacturonic acid content of M−IDF was superior to that of F-IDF, suggesting that the modification promoted the dissociation of pectin in the plant cell wall, and a higher pectin concentration enhanced the adsorption capacity of IDF (Qin et al., 2023). Arabinose, rhamnose, and glucose are typical components of hemicellulose (Gu et al., 2020), and the combined modification treatment accelerated the cleavage of cellulose, resulting in an increase in arabinose content. The main monosaccharides in the F-IDF were galactose, arabinose, and galacturonic acid. Compared to those of F-IDF, the glucose content of M−IDF was decreased, whereas the galactose, arabinose, and xylose contents were increased, owing to the effects of jet cavitation and cellulase. Simultaneously, the cellulose and

Table 2
Chemical composition, monosaccharide composition (g/100 g), and colour parameters of F-IDF and M−IDF were analysed.

Treatment	F-IDF	M−IDF
The yield of IDF (%)		
IDF	77.31 ± 0.19^{b}	64.32 ± 0.47^{a}
Chemical composition of IDFs (g/100 g Dry IDF)		
Moisture	4.29 ± 0.12^{Ab}	4.11 ± 0.04^{A}
Fat	3.40 ± 0.21^{Ab}	2.90 ± 0.20^{A}
Protein	3.49 ± 0.21^{b}	2.80 ± 0.07^{a}
Monosaccharide composition of different IDFs (%)		
Rha	5.26 ± 0.66^{A}	5.07 ± 0.35^{A}
Ara	18.79 ± 0.64^{A}	19.27 ± 0.13^{A}
Gal	43.30 ± 0.44^{b}	49.65 ± 0.22^{a}
Glu	17.61 ± 0.97^{Ab}	6.13 ± 0.19^{A}
Xyl	6.44 ± 0.17^{Ab}	7.43 ± 0.54^{A}
Man	1.63 ± 0.08^{A}	1.35 ± 0.02^{A}
Gala	7.01 ± 0.31^{b}	8.11 ± 0.91^{a}
Colour space parameters		
L*	88.01 ± 0.19^{A}	81.58 ± 0.33^{Ab}
a*	1.64 ± 0.01^{A}	0.95 ± 0.11^{Ab}
b*	14.25 ± 0.01^{A}	15.28 ± 0.24^{Ab}
Chroma	83.42 ± 0.01^{A}	86.44 ± 0.11^{Ab}
Hue	14.34 ± 0.01^{a}	15.31 ± 0.24^{b}

Results are presented as mean ± standard deviation (n = 3). Means of the same parameter in the same column with different lowercase superscript letters indicate significant differences ($P < 0.05$).

hemicellulose contents were reduced, which is similar to the results of previous studies (Sang et al., 2022). Thus, changes in the monosaccharide composition could thus change the microstructure and physicochemical functional properties (WHC, OHC, SC, and SAC) of the M−IDF samples.

3.2. FT-IR spectral analysis

To clarify the effect of jet cavitation combined with cellulase on the functional groups of IDF, the FT-IR spectra of F-IDF and M−IDF were obtained (Fig. 1A). The characteristic FT-IR absorption peaks of the two IDF samples were similar. The absorption peak positions and intensities of the IDF samples at 1600 cm^{-1} and 3430 cm^{-1} before and after modification were different, suggesting that the chemical structure of IDF remained largely unchanged after modification. The peaks at 3000–3700 cm^{-1} correspond to hydrogen bond regions. The peaks at 3200–3310 cm^{-1} correspond to intermolecular hydrogen bonds, whereas those at 3375–3455 cm^{-1} correspond to intramolecular hydrogen bonds (Luo et al., 2018).

Compared with that of F-IDF, the FTIR spectrum of M−IDF exhibited a significant red shift to 3435 cm^{-1} (corresponding to O—H vibration), and the peak intensity of M−IDF increased, indicating the formation of hydrogen bonds between cellulose molecules within the molecule and between water and cellulose molecules (Dong et al., 2021). The peaks at 2910–2935 cm^{-1} and 1620–1730 cm^{-1} showed the presence of –CH_2 and –COOH groups in the IDF. The weak peak at 1400–1415 cm^{-1} was attributed to the deformation band of polysaccharide methyl groups. M−IDF showed a weak peak at 1246 cm^{-1}, corresponding to the O—H or C—O group vibrations of hemicellulose (Xi et al., 2018), likely owing to the breakdown of cellulose into hemicellulose caused by jet cavitation and cellulase enzymatic hydrolysis. The peak at 900–1200 cm^{-1} was attributed to the stretching vibration of the CO-OR group in hemicellulose and the C—O group in lignin (Lyu et al., 2021). The peaks near 1629, 1246, and 1060 cm^{-1} of the M−IDF and F-IDF samples indicated the presence of uronic acid.

3.3. Functional characteristic analysis of IDF

We then evaluated the WHC, OHC, SC, and SAC of the two types of IDF (Fig. 1B-C), as these are closely related to intestinal health (Cui et al., 2019). The WHC of M−IDF (8.83 ± 0.17 g/g) was significantly higher than that of F-IDF (6.55 ± 0.25 g/g). This could be due to the combined effect of jet cavitation and cellulase hydrolysis, which enhances the porosity of the M−IDF surface, resulting in a porous and fluffy structure with additional exposed hydrophilic groups (Wu et al., 2020). The high WHC of IDF can change the viscosity of yoghurt and prevent shrinkage, promoting product stability by reducing whey precipitation and extending the shelf life. In addition, the WHC of the obtained M−IDF were significantly higher than those of alkaline hydrogen peroxide-modified congeners DF (4.07 ± 0.05 g/g) (Yan et al., 2023).

The OHC of the M−IDF (3.96 ± 0.03 g/g) was higher than that of the F-IDF because M−IDF (2.03 ± 0.15 g/g) has a larger specific surface area, increasing the porosity and attractiveness of the fibre and enhancing the physical encapsulation of the oil, increasing the OHC. Zhu

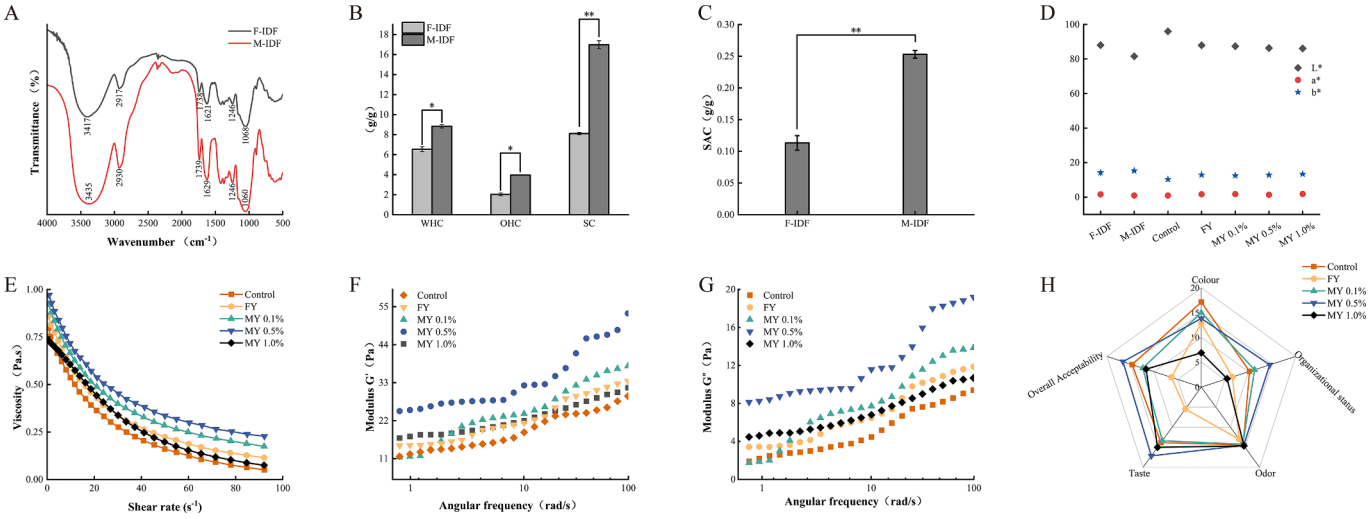

Fig. 1. (A) FTIR spectra of F-IDF and M−IDF, (B) WHC, OHC, and SC of F-IDF and M−IDF, (C) SAC of F-IDF and M−IDF, (D) colour parameters of IDF and IDF-added yoghurt: L* (brightness) a* (red) and b* (yellow). Rheological properties of yoghurt with IDF: (E) Effect of shear rate (0 ~ 1000 s^{-1}) on viscosity; (F) Relationship between storage modulus G′ and angular frequency (0.1 ~ 100 rad/s); (G) Relationship between loss modulus G‘‘ and angular frequency (0.1 ~ 100 rad/s); (H) Sensory evaluation. Histogram and scatter plot represent mean ± SD (standard deviation), and the difference between different letters was statistically significant ($P < 0.05$, n = 3). FY: add 0.5 % F-IDF yoghurt; MY 0.1 %: add 0.1 % M−IDF yoghurt; MY 0.5 %: add 0.5 % M−IDF yoghurt; MY 1.0 %: add 1.0 % M−IDF yoghurt. (For interpretation of the references to colour in this figure legend, the reader is referred to the web version of this article.)

et al. (2022) reported similar results. However, the co-modified M−IDF OHC was still higher than that of the shear emulsification-treated Lotus leaf DF (3.73 ± 0.17 g/g) (Zheng et al., 2023). Furthermore, The SC of M−IDF (16.98 ± 0.4 g/g) was significantly higher than that of F-IDF (8.11 ± 0.11 g/g), the increase in the SC of M−IDF could be attributed to its numerous complex porous structures, which facilitate the entry of water molecules into the cellulose interior and prevent their escape.

The SAC test results for the F-IDF and M−IDF (Fig. 1C) were consistent with those of the OHC, revealing that M−IDF exhibited the highest adsorption capacity for bile salts (0.25 ± 0.06 g/g). This effect is due to cavitation and enzymatic hydrolysis. Under these conditions, the hydrogen bonds between the long chains of the molecules are broken, leading to the exposure of short-chain molecules and more groups on the surface; the surface of the IDF has a rough and porous structure. As the number of lipophilic groups increases, the SAC of the M−IDF improves (Si et al., 2023). Compared to that of F-IDF, the SAC of M−IDF significantly increased by 2.27-fold, indicating that combining jet cavitation with cellulase effectively enhanced the SAC of IDF. Meanwhile, the SAC of M−IDF was significantly lower than that of *Aspergillus niger* coenzyme-modified shiitake DF (0.87 ± 0.28 mg/g) (Si et al., 2023). These results suggest that IDF modified by combining jet cavitation and cellulase may be a functional food additive with excellent WHC and lipid-lowering properties.

3.4. Microstructure analysis

Different preparation methods had different effects on the physical structures of the IDF samples, affecting their functional properties. Fig. 2 shows the F-IDF and M−IDF microstructural characteristics, as observed through SEM analysis. The F-IDF tissue samples appeared complete, flaky, and wrinkled (Fig. 2A). However, Fig. 2B shows that the surface of M−IDF was rough, irregular, and cracked owing to the combined action of cavitation, high temperature, high pressure, and enzymatic hydrolysis, which could improve the properties of WHC compared to those of F-IDF. We previously found that the effect of enzymatic modification alone on the microstructure of IDF was minimal. However, enzymatic modification and jet cavitation effectively opened the dense structure of the IDF, increasing the contact area between the enzyme and IDF (Tian et al., 2023). The surface structure, area, and porosity of IDF affect some of its physical and chemical properties, which could explain the physiological benefits of modified M−IDF, such as blood lipid-lowering and fat-adsorption effects (Wu et al., 2020).

The microstructure of yoghurt is mainly composed of casein micelle networks with irregular shapes and internal voids (Wang et al., 2020). The control yoghurt sample had a continuous protein chain and a pore network structure (Fig. 2C). F-IDF and different amounts of M−IDF were added, and their combination with the protein network was observed via SEM (Fig. 2D, E, F, and G). Fig. 2D shows that F-IDF effectively reduced the pore network structure of yoghurt. However, compared to the results shown in Fig. 2E, 2F, and 2G, the improving effect of F-IDF was not significant. This indicates that M−IDF and casein micelles effectively decreased the pore network structure through electrostatic and hydrophobic interactions within a pH range of 3.8–4.5 (Dong et al., 2021). This microscopic structure can minimise protein rearrangement and sensitivity to dehydration shrinkage, enhancing yoghurt stability containing varying amounts of M−IDF during storage (Fig. 2A). The SEM data presented here are consistent with previous research on DF-supplemented yoghurt (Varnaitė et al., 2022). Furthermore, the intricate micelle network structure formed via adsorbed M−IDF and casein aggregation contributes to the overall yoghurt stability (Fan et al., 2023).

3.5. Colour analysis

Colour is the most direct factor that attracts consumers, and the first to be perceived; thus, colour is important in decision-making. Table 2 shows the colour parameters (L *, a *, b *, chroma, hue) of the two IDF and IDF-added yoghurt samples. The L* parameter of the M−IDF decreased significantly (Fig. 1D), indicating that the structure of natural pigments may be degraded under modified conditions (Azucena et al., 2023). The a* parameter of the M−IDF was lower, than that of F-IDF, whereas the b* parameter was higher. The F-IDF and M−IDF chroma values were 83.42 ± 0.01 and 86.44 ± 0.11 (yellowish), respectively.

For yoghurt containing F-IDF and different amounts of M−IDF, the colour of the MY group changed significantly according to the amount of M−IDF added. Compared to those of the control yoghurt, the a* and b* values of F-IDF or M−IDF increased significantly (Table S3), and the L* value decreased significantly (Fig. 1D). Compared to the FY group, the L* value in the MY group decreased significantly with an increase in the amount of yoghurt added, whereas the a* and b* values increased significantly. Dong et al., 2021 reported similar results for yoghurt containing carrot DF. Concurrently, the MY 1.0 % group had significantly higher b* values and colouration than the control group (b* = 13.34 ± 0.35, chroma = 13.47 ± 0.33). Therefore, by detecting the L*, a*, b*, chroma, and hue of different yoghurt samples, the addition of different amounts of M−IDF was found to have a significant effect, mainly because of the higher b* value of M−IDF.

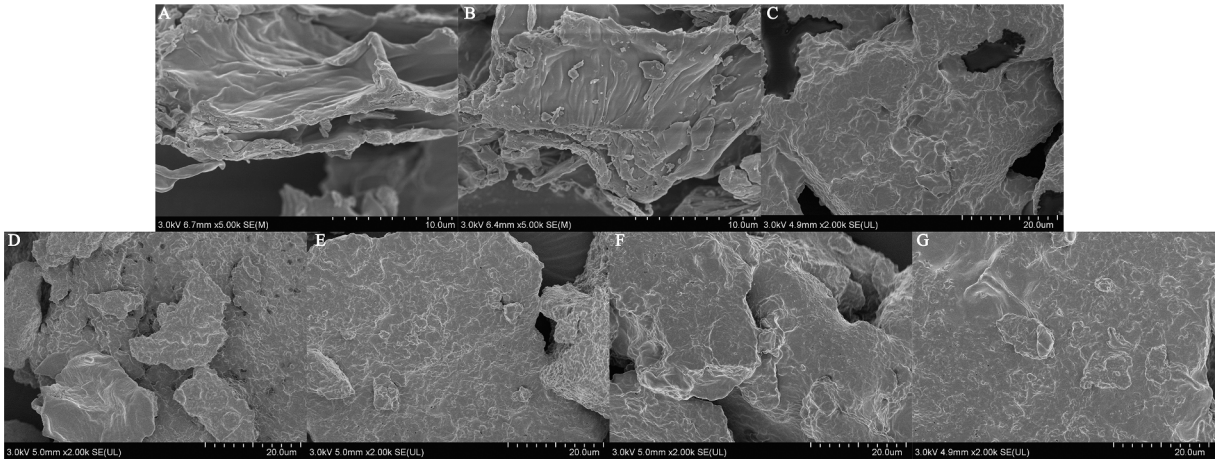

Fig. 2. SEM micrographs of different IDF: F-IDF (A), M−IDF (B) and yoghurt with IDF: Control (C), FY (D), MY 0.1 % (E), MY 0.5 % (F), MY 1.0 % (G). FY: add 0.5 % F-IDF yoghurt; MY 0.1 %: add 0.1 % M−IDF yoghurt; MY 0.5 %: add 0.5 % M−IDF yoghurt; MY 1.0 %: add 1.0 % M−IDF yoghurt.

3.6. Changes in total and reducing sugar content in yoghurt during storage

The changes in total sugar and reducing sugar content in the five groups of different yoghurts during the 21-day storage period are shown in Table S4. According to the data in Table S4, the total sugar content of the MY 1.0 % group was significantly higher than that of the control, FY, MY 0.1 %, and MY 0.5 % groups during each storage period. The reducing sugar content of the FY group was significantly higher than that of the control, MY 0.1 %, MY 0.5 %, and MY 1.0 % groups, similar to the monosaccharide composition (Table 2). Extracellular polysaccharides of lactic acid bacteria produced by the fermentation of lactic acid bacteria in yoghurt during storage also influence changes in total sugar content during storage (Yang et al., 2023). Glucose is a reducing sugar. Monosaccharide composition analysis showed that F-IDF contained a large amount of glucose, which increased the reducing sugar content in yoghurt, indicating that IDF contains certain polysaccharides and reducing sugars, increasing the nutritional components of yoghurt. During the 21-day storage period, the total sugar and reducing sugar content of different yoghurt groups gradually decreased, as sugar was the main carbon source for microbial growth (Xu et al., 2023).

3.7. pH, TA, and whey separation rate of yoghurt

TA affects the viability of probiotics during yoghurt production and storage, and affects their quality. During the storage period, the acid–base values of all yoghurt types were between 3.87 and 4.48 (Table S4). These changes may be related to bacterial metabolism that breaks down dietary fibre to produce lactic acid and other organic acids during yoghurt fermentation and storage (Kumari et al., 2023). During the 21 days of low-temperature storage, the pH of yoghurt containing okara F-IDF and different concentrations of M−IDF was lower than that of the control yoghurt (Table S4). On the day 21, the pH of MY 1.0 % reached its lowest value compared to that of the other yoghurt groups. The TA value of each group increased with a decrease in pH ($P < 0.05$). Emun et al. (2016) reported similar results. The titratable acidity of yoghurt in the MY0.5 % group during storage was significantly higher than that of yoghurt supplemented with microwave-modified carrot DF (0.87–1.13) (Dong et al., 2022). The decrease in pH and increase in TA during storage were caused by the large amount of lactic acid produced by the lactic acid bacteria.

Dehydration shrinkage is an undesirable feature that involves whey accumulation on the yoghurt surface (Hanna et al., 2020). Furthermore, the addition of IDF significantly reduced dehydration shrinkage during low-temperature storage at 4 °C ($P < 0.05$) because IDF strengthened the tight junctions of the internal structure, which might be related to the adsorption of whey casein by the IDF to form a gel during the water-binding process (Fan et al., 2022). In addition, the whey precipitation rate of yoghurt in the MY0.5 % group was significantly lower than that in the whey precipitation rate of yoghurt with the addition of 1 % rice bran (42.6 ± 1.84) (Demirci et al., 2017). During storage, the whey precipitation rate of MY 0.5 % was the lowest (Table S4), followed by that of MY 1.0 %. The adsorption capacity of the modified IDF was enhanced and the pectin content was higher, which increased the viscosity of M−IDF in the yoghurt liquid and reduced the release of whey. In addition, electrostatic and spatial interactions between M−IDF and casein complexes during yoghurt fermentation further enhance the protein gel network constituted by casein aggregates, with a consequent reduction in whey precipitation (Sodini et al., 2020, Kumari et al., 2023).

3.8. Analysis of rheological properties of yoghurt

Food rheology involves studying food deformation under the action of force. Determining the rheological properties of food is important for identifying and controlling its quality (Fu et al., 2021). As shown in Fig. 1E, the apparent viscosity of all yoghurt samples gradually decreased with increasing shear rate. Additionally, the curve sloped downward, indicating that all yoghurt samples exhibited pseudoplastic fluid behaviour, which is also known as shear-thinning fluid (Dong et al., 2021). This may be due to the increase in shear rate, which causes the protein molecules to gradually move in the same direction, and the intermolecular interaction forces to decrease, leading to the breakage of chemical bonds, such as hydrogen bonding and dissociation of proteins (Fan et al., 2023). Among all yoghurt groups, the viscosity and shear force in the MY 0.5 % group were significantly higher than those in the other groups (MY 0.5 % > MY 0.1 % > FY > MY 1.0 % > control).

The rough surface structure of the modified M−IDF might have caused this result, as it reduced the particle size, increased the surface area, and enhanced its interaction with casein particles, thereby increasing the viscosity of yoghurt (Tian et al., 2023; Ma et al., 2019). Conversely, compared to that observed in the control group, the addition of F-IDF or M−IDF modified the total solids and other components of yoghurt, impacting its rheological properties. Similar findings have been reported for yoghurt fortified with apple pomace (Wang et al., 2020). M−IDF powder dispersed in the yoghurt matrix can significantly increase the viscosity, which is affected by the amount of M−IDF added and its internal structure, functional properties, and composition. M−IDF demonstrated significant WHC, SC, and thickening ability (related to the total sugar content), improving the viscosity of yoghurt.

G′ represents the stress generated by the deformation of the sample during impact, and is a measure of sample elasticity. G″ represents the energy lost during yoghurt deformation and is used to measure yoghurt viscosity (Fan et al., 2023). G′ > G″ indicates that the sample exhibits colloidal viscoelastic behaviour. Fig. 1F and G show the relationship between G′ and G“ and the angular frequency (0.1–100 rad/s) in the control and F-IDF or M−IDF yoghurt samples. The five types of yoghurt showed linear viscoelastic behaviour with angular frequencies of 1–100 rad/s. The G′ values of all samples were greater than the G′ values at low amplitudes, indicating that the colloidal structures of these samples were weakly curled. Similar results have been obtained for the rheological properties of potato DF in yoghurt (Ahmad et al., 2021). After adding okara F-IDF or M−IDF, G′ and G″ increased significantly, indicating that IDF was involved in forming the whole-protein gel network. The G′ of M−IDF 0.5 % was the highest, followed by that of MY-IDF 0.1 %. The results for the G′ and G″ showed the same trend (Fig. S3F and Fig. S3G), indicating that the viscosity of the M−IDF samples was higher, suggesting that the interaction between M−IDF and casein particles might be stronger than that with F-IDF.

3.9. Yoghurt texture analysis

Yoghurt texture is an important factor influencing consumer acceptance. There were significant differences in hardness, elasticity, cohesion, and stickiness between yoghurt in the FY and MY 0.5 % groups ($P < 0.05$) (Table S3). Addition of 0.5 % M−IDF significantly yoghurt hardness (18.76 ± 0.19 N), elasticity (0.95 ± 0.04) and cohesion (0.95 ± 0.17). Yoghurt hardness is directly related to the total solid content of the milk mixture (Tatdao et al., 2008) and increases with the addition of M−IDF at concentrations of 0.1 %, 0.5 %, and 1.0 % (m/w). The MY 0.5 % group showed a significantly greater hardness than the control group, similar to the results obtained by Pang et al. (2017) when tilapia skin gelatine was added as a stabiliser. The gumminess results were consistent with the apparent viscosity data, reinforcing the thickening effect of M−IDF.

The cohesiveness reflects the degree of deformation of a material before fracture and is directly related to the internal strength of the material structure (Alsop et al., 1997). The increase in cohesiveness of yoghurt containing M−IDF may be due to the higher viscosity of M−IDF, which enhances the internal gel structure. Moreover, M−IDF powder can adsorb whey and casein from yoghurt, thus strengthening the original loose and open protein structure. The increase in the viscosity of yoghurt containing guar gum can be attributed to gelation and

interaction between guar gum and casein micelles in milk (Lee et al. 2016). This gelation and interaction depended on the concentration of guar gum added, similar to our results.

3.10. Sensory evaluation

The yoghurt structure and composition influence its flavour. Moreover, the product structure affects the migration of aromatic compounds to the top of the product, and the addition of IDF before and after modification had different effects on the microstructure and sensory properties of yoghurt. Yoghurt in the MY 0.5 % group had the highest scores for tissue morphology (14.5 ± 1.31), odour (14.53 ± 1.11), and taste (17.13 ± 0.86), whereas all yoghurt containing IDF had a light-yellow colour, possibly due to the residual major isoflavone daidzein in IDF (Fig. 1H). Daidzein can ameliorate obesity in animals (Khatun et al., 2023). The organisation score of MY 0.5 % yoghurt (14.5) was higher ($P < 0.05$) than that of the control (10.23) and FY groups (6.6) because it had a uniform texture and no whey precipitation, which was consistent with the texture and rheological results (Fig. 1E, F, and G; Table S4), indicating that M−IDF can improve the yoghurt texture. M−IDF addition significantly affected the odour score, resulting in a special flavour that coincided with the milk flavour. This phenomenon could be due to the increased use of IDF and protein by probiotics during fermentation, resulting in relatively high concentrations of flavour substances such as acetone, acetaldehyde, diacetyl, and acetic acid (Fan et al., 2023). The taste score of the M−IDF group (17.13) was higher than that of the control (13.83) and FY groups (5.47), indicating a delicate and elastic taste. The acid-reducing effect of M−IDF in yoghurt and the good aroma and texture after adding 0.5 % M−IDF affected taste evaluation. Therefore, the addition of 0.5 % M−IDF was generally acceptable to consumers.

3.11. Changes in the antioxidant capacity of yoghurt during storage

Fig. S3 shows the changes in DPPH• scavenging ability, ABTS•$^{+}$ scavenging ability, and *T*-AOC activity of yoghurt in the control, FY, MY 0.1 %, MY 0.5 %, and MY 1.0 % groups during different storage periods. The DPPH•, ABTS•$^{+}$, and *T*-AOC scavenging activities of all M−IDF fortified yoghurt samples were significantly reduced in a dose-dependent manner ($P < 0.05$), and continued to decrease throughout the storage period (Fig. S3A-C).

After storage, the DPPH• scavenging rate (20.77 %), ABTS•$^{+}$ scavenging rate (49.67 %), and *T*-AOC activity (3.1 mmol/L) of yoghurt with 1.0 % M−IDF were the highest. The antioxidant activity potential of M−IDF yoghurt was consistent with previous reports on the effect of adding mushroom polysaccharide yoghurt (Radzki et al., 2023). On day 1, yoghurt from the MY1% group was significantly higher than yoghurt from 1 % rice bran in terms of DPPH-radical scavenging and ABTS-+ radical scavenging (5.6 ± 0.54 %, 0.78 ± 0.01 %) (Demirci et al., 2017). This phenomenon may be due to the following reasons: (a) compared with F-IDF, M−IDF can be used as a good electron donor to provide hydrogen, thereby removing free radicals and preventing a free radical chain reaction (Li et al., 2022); (b) polysaccharides in dietary fibre can increase the activity of antioxidant enzymes such as superoxide dismutase (SOD), catalase (CAT), and glutathione peroxidase (GSH-PX) (Huang et al., 2017); and (c) the antioxidant activity of dietary fibre is related to its monosaccharide composition, glycosidic bond connection mode, and structural conformation (Simas et al., 2010; Qiao et al., 2021).

During storage, M−IDF is partially degraded into SDF after fermentation by lactic acid bacteria. SDF modified by lactic acid bacteria have a high antioxidant capacity (Li et al., 2022). In contrast, yoghurt has antioxidant properties, which can produce antioxidant-active substances such as SOD, GSH-PX, CAT, NADH oxidase, metallothionein, among others (Huang et al., 2017). Adding dietary fibre can increase the number of microorganisms and the production of active substances. For example, extracellular polysaccharides secreted by lactic acid bacteria have good antioxidant effects (Zhou et al., 2023). Notably, the antioxidant activity of yoghurt in the control group also slowly decreased during the storage period. Fermented metabolites such as peptides, free amino acids, fatty acids, and enzymes may have the potential for redox balance, which can enhance the antioxidant capacity of yoghurt (Sah et al., 2014). These results showed that adding M−IDF effectively improved the free radical scavenging ability of yoghurt and prolonged its shelf life.

4. Conclusion

Here, the structural and functional properties of IDF were investigated using jet cavitation combined with cellulase modification. As the results show, combining the two methods can make the surface of the IDF rougher, with more irregular and cracked lamellar structures, and can increase the polysaccharide content. Thus, IDF has a higher water-holding, oil-holding, and bile salt-adsorption capacities. We also studied the effects of IDF on the microstructure, rheological properties, and storage stability of yoghurt after fermentation. Adding 0.5 % modified IDF to yoghurt combined with casein reduces the pore network structure and improves the whey precipitation rate, rheological properties, and texture. Simultaneously, the modified IDF provides a suitable pH value for the survival of yoghurt probiotics during storage, prolonging the shelf life and giving the yoghurt a yellowish colour, which improves its sensory effect. It reduces the decrease in antioxidant activity during storage to a large extent. Therefore, jet cavitation combined with cellulase-modified okara IDF may improve yoghurt quality, providing a theoretical basis for developing functional IDF-rich foods. There are still many shortcomings in this study: the interaction between M−IDF and yoghurt protein should be discussed in more detail, and the detailed mechanism of action should be obtained.

Sensory evaluation consent statement

The sensory evaluation used in this study was approved by the Institutional Review Board of Heilongjiang Bayi Nongken University. The rights and privacy of all participants are fully protected during the implementation of the study. Each participant is fully aware of the requirements of this study and the potential risks that may arise, and with the verbal consent of all participants, participants ' data are not released without their knowledge.

CRediT authorship contribution statement

Yu Tian: Conceptualization, Investigation, Methodology, Writing – original draft. **Yanan Sheng:** Conceptualization, Data curation, Investigation, Resources, Validation, Writing – review & editing. **Tong Wu:** Data curation, Methodology, Writing – review & editing. **Changyuan Wang:** Funding acquisition, Resources, Supervision, Writing – review & editing.

Declaration of competing interest

The authors declare that they have no known competing financial interests or personal relationships that could have appeared to influence the work reported in this paper.

Data availability

Data will be made available on request.

Acknowledgments

This work was supported by the Heilongjiang province “millions of” project science and technology major special project (2021ZX12B02)

and Heilongjiang Bayi Agricultural University Graduate Innovative Research Project (YJSCX2022-Y44).

Appendix A. Supplementary data

Supplementary data to this article can be found online at https://doi.org/10.1016/j.fochx.2023.101064.

References

Ahmad, I., Xiong, Z. Y., Xiong, H. G., Khalid, N., & Rasul, S. H. A. (2021). Effect of enzymatically hydrolyzed potato powder on quality characteristics of stirred yogurt during cold storage. *Journal of Food Processing and Preservation, 45*(9), e15690. https://10.1111/jfpp.15690.

Alsop, S., Matchett, A. J., Coulthard, J. M., & Peace, J. (1997). Elastic and cohesive properties of wet particulate materials. *Powder Technology, 91*(2), 157–164. https://10.1016/s0032-5910(96)03257-3.

Azucena, R. M., Araceli, O. M., Marina, G. H., Miriam, R. Q., Francisco, G. L., & Begoña, O. A. (2023). Natural pigments of plant origin: Classification, extraction and application in foods. *Food Chemistry, 398*, 1. https://10.1016/j.foodchem.2022.133908.

Cui, J. F., Lian, Y. H., Zhao, C. Y., Du, H. J., Han, Y. H., Gao, W., et al. (2019). Dietary Fibers from Fruits and Vegetables and Their Health Benefits via Modulation of Gut Microbiota. *Comprehensive Reviews in Food Science and Food Safety, 18*(5), 1514–1532. https://10.1111/1541-4337.12489.

Demirci, T., Aktaş, K., Sözeri, D., Öztürk, H.İ., & Akın, N. (2017). Rice bran improve probiotic viability in yoghurt and provide added antioxidative benefits. *Journal of Functional Foods, 36*, 396–403. https://doi.org/10.1016/j.jff.2017.07.019

Dong, R. H., Liao, W., Xie, J. H., Chen, Y., Peng, G. Y., Xie, J. Y., et al. (2021). Enrichment of yogurt with carrot soluble dietary fiber prepared by three physical modified treatments: Microstructure, rheology and storage stability. *Innovative Food Science & Emerging Technologies, 75*. https://10.1016/j.ifset.2021.102901.

Emun, K., Eyassu, S., Geremew, B., & Solomon, W. K. (2016). Effect of carrot juice and stabilizer on the physicochemical and microbiological properties of yoghurt. *LWT - Food Science and Technology, 69*, 191–196. https://10.1016/j.lwt.2016.01.026.

Fan, X. K., Li, X. F., Du, L. H., Li, J. H., Xu, J., Shi, C. W., et al. (2022). The effect of natural plant based homogenates as additives on the quality of yogurt: A review. *Food Bioscience, 49*, Article 101953. https://10.1016/j.fbio.2022.101953.

Fan, X. K., Shi, Z. H., Xu, J., Li, C. W., Li, X. F., Jiang, X. X., et al. (2023). Characterization of the effects of binary probiotics and wolfberry dietary fiber on the quality of yogurt. *Food Chemistry, 406*, Article 135020. https://10.1016/j.foodchem.2022.135020.

Gan, J. P., Xie, L., Peng, G. Y., Xie, J. H., Chen, Y., & Yu, Q. (2021). Systematic review on modification methods of dietary fiber. *Food Hydrocolloids, 119*, 1068721. https://10.1016/j.foodhyd.2021.106872.

Gu, M., Fang, H., Gao, Y., Su, T., Niu, Y., & Yu, L. (2020). Characterization of enzymatic modified soluble dietary fiber from tomato peels with high release of lycopene. *Food Hydrocolloids, 99*, Article 105321. https://doi.org/10.1016/j.foodhyd.2019.105321

Hanna, L., Cécile, R., Marie, F., Saïd, B., & Carole, P. (2020). Yogurts enriched with milk proteins: Texture properties, aroma release and sensory perception. *Trends in Food Science & Technology, 98:(140–149)*. https://doi.org/10.1016/j.tifs.2020.02.006

Huang, G. L., Mei, X. Y., & Hu, J. C. (2017). The Antioxidant Activities of Natural Polysaccharides. *Current drug targets* (11). https://10.2174/1389450118666170123145357.

Khatun, S., Kim, T., & Mollah, M. M. I. (2023). Heat shock increases the anti-inflammatory and anti-obesity activity of soybean by increasing polyphenol, antioxidant and aglycon form isoflavones. *Heliyon. https://*. https://doi.org/10.1016/j.heliyon.2023.e21944

Kumari, T., Das, A. B., & Deka, S. C. (2023). Effect of enzymatic modified pea peel dietary fibre on syneresis, texture, rheology and microstructural properties of yogurt. *Biomass Conversion and Biorefinery, 1–13*. https://doi.org/10.1007/s13399-023-04933-z

Li, Y. X., Niu, L., Guo, Q. Q., Shi, L. C., Deng, X., Liu, X. B., et al. (2022). Effects of fermentation with lactic bacteria on the structural characteristics and physicochemical and functional properties of soluble dietary fiber from prosomillet bran. *LWT*. https://doi.org/10.1016/j.lwt.2021.112609

Luo, X. L., Wang, Q., Fang, D. Y., Zhuang, W. J., Chen, C. H., Jiang, W. T., et al. (2018). Modification of insoluble dietary fibers from bamboo shoot shell: Structural characterization and functional properties. *International Journal of Biological Macromolecules, 120*(Pt B), 1461–1467. https://10.1016/j.ijbiomac.2018.09.149.

Lyu, B., Wang, H., Swallah, M. S., Fu, H. L., Shen, Y., Guo, Z. W., et al. (2021). Structure, properties and potential bioactivities of high-purity insoluble fibre from soybean dregs (Okara). *Food Chemistry, 364*, Article 130402. https://10.1016/j.foodchem.2021.130402.

Ma, Y. S., Zhao, H. J., & Zhao, X. H. (2019). Comparison of the Effects of the Alcalase-Hydrolysates of Caseinate, and of Fish and Bovine Gelatins on the Acidification and Textural Features of Set-Style Skimmed Yogurt-Type Products. *Foods, 8*(10), 501. https://10.3390/foods8100501.

Miocinovic, J., Tomic, N., Dojnov, B., Tomasevic, I., Stojanovic, S., Djekic, I., et al. (2018). Application of new insoluble dietary fibres from triticale as supplement in yoghurt - effects on physico-chemical, rheological and quality properties. *Journal of the science of food and agriculture, 98*(4), 1291–1299. https://10.1002/jsfa.8592.

Pang, Z. H., Deeth, H., Yang, H. S., Prakash, S., & Nidhi, B. (2017). Evaluation of tilapia skin gelatin as a mammalian gelatin replacer in acid milk gels and low-fat stirred yogurt. *Journal of Dairy Science, 100*(5), 3436–3447. https://10.3168/jds.2016-11881.

Qiao, C. C., Zeng, F. K., Wu, N. N., & Tan, B. (2021). Functional, physicochemical and structural properties of soluble dietary fiber from rice bran with extrusion cooking treatment. *Food Hydrocolloids. https://*. https://doi.org/10.1016/J.FOODHYD.2021.107057

Qin, X., Yang, C., Si, J., Chen, Y., Xie, J., Tang, J., et al. (2023). Fortified yogurt with high-quality dietary fiber prepared from the by-products of grapefruit by superfine grinding combined with fermentation treatment. *LWT, 188*, Article 115396. https://doi.org/10.1016/j.lwt.2023.115396

Radzki, W., Skrzypczak, K., Sołowiej, B., Jabłońska-Ryś, E., & Gustaw, W. (2023). Properties of Yogurts Enriched with Crude Polysaccharides Extracted from Pleurotus ostreatus Cultivated Mushroom. *Foods, 12*(21), 4033. https://10.3390/foods12214033.

Sah, B. N. P., Vasiljevic, T., McKechnie, S., & Donkor, O. N. (2014). Effect of probiotics on antioxidant and antimutagenic activities of crude peptide extract from yogurt. *Food Chemistry*. https://doi.org/10.1016/j.foodchem.2014.01.105

Sang, J. Q., Li, L., Wen, J., Liu, H. C., Wu, J. J., Yu, Y. S., et al. (2022). Chemical composition, structural and functional properties of insoluble dietary fiber obtained from the Shatian pomelo peel sponge layer using different modification methods. *LWT, 165*, Article 113737. https://10.1016/j.lwt.2022.113737.

Si, J. Y., Yang, C. R., Chen, Y., Xie, J. H., Tian, S. L., Cheng, Y. N., et al. (2023). Structural properties and adsorption capacities of Mesona chinensis Benth residues dietary fiber prepared by cellulase treatment assisted by Aspergillus niger or Trichoderma reesei. *Food Chemistry, 407*, Article 135149. https://10.1016/j.foodchem.2022.135149.

Simas, K. N., Vieira, L. D. N., Podestá, R., Vieira, M. A., Rockenbach, I. I., Petkowicz, C. L., et al. (2010). Microstructure, nutrient composition and antioxidant capacity of king palm flour: A new potential source of dietary fibre. *Bioresource technology, 101*(14), 5701–5707. https://doi.org/10.1016/j.biortech.2010.02.053

Tatdao, P., Darryl, M. S., & Frank, S. (2008). Rheology and texture of set yogurt as affected by inulin addition. *Journal of Texture Studies, 39*(6), 617–634. https://10.1111/j.1745-4603.2008.00161.x.

Tian, M. L., Pak, S. J., Ma, C., Ma, L. J., Rengasamy, K. R., Xiao, J., et al. (2022). Chemical features and biological functions of water-insoluble dietary fiber in plant-based foods. *Critical reviews in food science and nutrition. https://*. https://doi.org/10.1080/10408398.2022.2110565

Tian, Y., Wu, T., Sheng, Y. N., Li, L. N., & Wang, C. Y. (2023). Effects of cavitation-jet technology combined with enzyme treatment on the structure properties and functional properties of OKARA insoluble dietary fiber. *Food Chemistry, 423*, Article 136286. https://10.1016/j.foodchem.2023.136286.

Varnaitė, L., Keršienė, M., Šipailienė, A., Kazernavičiūtė, R., Venskutonis, P., & Leskauskaitė, D. (2022). Fiber-Rich Cranberry Pomace as Food Ingredient with Functional Activity for Yogurt Production. *Foods, 11*(5), 758. https://10.3390/foods11050758.

Wang, X. Y., Kristo, E., & Gisèle, L. P. (2020). Adding apple pomace as a functional ingredient in stirred-type yogurt and yogurt drinks. *Food Hydrocolloids, 100*(C), Article 105453. https://10.1016/j.foodhyd.2019.105453.

Wu, C. L., Teng, F., McClements, D. J., Zhang, S., Li, Y., & Wang, Z. J. (2020). Effect of cavitation jet processing on the physicochemical properties and structural characteristics of okara dietary fiber. *Food Research International, 134*, Article 109251. https://10.1016/j.foodres.2020.109251.

Wu, C. L., He, M. Y., Zheng, L., Tian, T., Teng, F., & Li, Y. (2021). Effect of cavitation jets on the physicochemical properties and structural characteristics of the okara protein. *Journal of food science, 86*(10), 4566–4576. https://10.1111/1750-3841.15891.

Xi, H. H., Wang, A. X., Qin, W. Y., Nie, M. Z., Chen, Z. Y., He, Y., et al. (2023). The structural and functional properties of dietary fibre extracts obtained from highland barley bran through different steam explosion-assisted treatments. *Food Chemistry, 406*, Article 135025. https://10.1016/j.foodchem.2022.135025.

Xu, X. Y., Cui, H. T., Xu, J. X., Yuan, Z. H., Li, J., Yang, L. N., et al. (2023). Effects of cold storage time on the quality and active probiotics of yogurt fermented by Bifidobacterium lactis and commercial bacteria Danisco. *Journal of food science. https://*. https://doi.org/10.1111/1750-3841.16601

Yan, K., Liu, J., Yan, W., Wang, Q., Huo, Y., Feng, S., et al. (2023). Effects of Alkaline Hydrogen Peroxide and Cellulase Modifications on the Physicochemical and Functional Properties of Forsythia suspensa Dietary Fiber. *Molecules, 28*(20), 7164. https://doi.org/10.3390/molecules28207164

Yang, X., Dai, J., Zhong, Y., Wei, X., Wu, M., Zhang, Y., et al. (2021). Characterization of insoluble dietary fiber from three food sources and their potential hypoglycemic and hypolipidemic effects. *Food & Function, 12*(14). https://10.1039/d1fo00521a.

Yang, Y., Jiang, G., & Tian, Y. (2023). Biological activities and applications of exopolysaccharides produced by lactic acid bacteria: A mini-review. *World Journal of Microbiology and Biotechnology, 39*(6), 155. https://doi.org/10.1007/s11274-023-03610-7

Zheng, H., Sun, Y., Zheng, T., Zeng, Y., Fu, L., Zhou, T., et al. (2023). Effects of shear emulsifying/ball milling/autoclave modification on structure, physicochemical properties, phenolic compounds, and antioxidant capacity of lotus (Nelumbo) leaves dietary fiber. *Frontiers in Nutrition, 10*, 1064662. https://doi.org/10.3389/fnut.2023.1064662

Zhou, D. P., Liu, J., Liu, S. W., Liu, X., Tang, X. Z., & Lv, X. Z. (2020). Characterization of alkaline and enzymatic modified insoluble dietary fiber from Undaria pinnatifida.

International Journal of Food Science & Technology, 55(12), 3533–3541. https://10.1111/ijfs.14686.

Zhou, Z. F., Zeng, X. Q., Wu, Z., Guo, Y. X., & Pan, D. D. (2023). Relationship of Gene-Structure-Antioxidant Ability of Exopolysaccharides Derived from Lactic Acid Bacteria: A Review. *Journal of agricultural and food chemistry*. https://doi.org/10.1021/acs.jafc.3c00532

Zhu, Y. L., Ji, X. L., Yuen, M., Yuen, T., Yuen, H., Wang, M., et al. (2022). Effects of Ball Milling Combined With Cellulase Treatment on Physicochemical Properties and in vitro Hypoglycemic Ability of Sea Buckthorn Seed Meal Insoluble Dietary Fiber. *Frontiers in Nutrition, 8*, Article 820672. https://10.3389/fnut.2021.820672.